



Natural time analysis: On the deadly Mexico M8.2 earthquake on 7 September 2017

Nicholas V. Sarlis^{a,*}, Efthimios S. Skordas^a, Panayiotis A. Varotsos^a,
Alejandro Ramírez-Rojas^b, E. Leticia Flores-Márquez^c

^a Section of Solid State Physics and Solid Earth Physics Institute, Department of Physics, National and Kapodistrian University of Athens, Panepistimiopolis, Zografos 157 84, Greece

^b Departamento de Ciencias Básicas, Universidad Autónoma Metropolitana, Azcapotzalco, Mexico, Mexico

^c Instituto de Geofísica, Universidad Nacional Autónoma de México, México

HIGHLIGHTS

- Natural time reveals precursory order parameter fluctuations in Mexico's seismicity.
- The entropy change under time reversal minimizes 3 months before the M8.2 earthquake.
- The M8.2 quake occurred in a region where the probability for extreme events was highest.

ARTICLE INFO

Article history:

Received 8 January 2018

Received in revised form 10 March 2018

Keywords:

Mexico earthquakes

Natural time

Entropy change under time reversal

Cocos and North American plates

ABSTRACT

A widespread opinion appears to prevail that the two recent deadly Mexico earthquakes, i.e., M8.2 on 7 September 2017 and M7.1 on 19 September 2017, in Chiapas and Morelos regions, respectively, had an unusual cause. Here, upon considering the analysis of seismicity in the new time domain termed natural time, we show that the occurrence of the M8.2 earthquake, which is Mexico's largest earthquake in more than a century, should not be considered unexpected. In particular, this analysis revealed well in advance that in Chiapas region, where the M8.2 earthquake occurred, the probability for the occurrence of an extreme event was the highest compared to other regions in Mexico. Furthermore, in this region, the investigation of the entropy change of seismicity under time reversal identified that almost 3 months before the occurrence of this major earthquake, an extreme event was likely to take place there.

© 2018 Elsevier B.V. All rights reserved.

1. Introduction

The magnitude M8.2 earthquake that struck the Mexico's Chiapas state on 7 September 2017 is Mexico's largest quake in more than a century. It left dozens dead and destroyed or severely damaged the homes of 2.3 millions or more. Most big Mexican earthquakes occur right along the interface between subducting Cocos plate and North American plate. But in this case the earthquake occurred within the Cocos plate itself (Fig. 1). The rupture began at 70 kilometer depth and rose up before stopping at about 40 kilometer depth, likely at the plate interface [1]. Some seismologists say this type of faulting would not produce such large earthquakes [2] and this is why they characterize it as an "extremely strange" event [1].

* Corresponding author.

E-mail addresses: nsarlis@phys.uoa.gr (N.V. Sarlis), eskordas@phys.uoa.gr (E.S. Skordas), pvaro@otenet.gr (P.A. Varotsos), arr@correo.azc.uam.mx (A. Ramírez-Rojas), leticia@geofisica.unam.mx (E.L. Flores-Márquez).

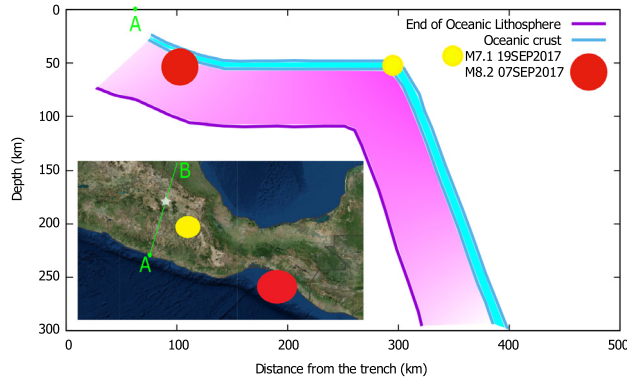


Fig. 1. A vertical cross-section of the Mexican flat-slab (along the direction AB shown in the inset, the position of point A is also shown on the upper horizontal axis) based on Refs. [5,42] together with the projection of the hypocenters of the two earthquakes on 7 September (red) and 19 September 2017 (yellow). The cyan surface depicts the oceanic crust while the magenta one the oceanic lithosphere. In the inset, we depict the epicenters of the two earthquakes superimposed on the ESRI World Imagery Base Map available from <https://worldmap.harvard.edu/maps/new>. The gray star shows Mexico city whereas point A is at Acapulco. (For interpretation of the references to color in this figure legend, the reader is referred to the web version of this article.)

Almost 12 days later, a M7.1 earthquake struck central Mexico on 19 September, killing more than 300 people and reducing buildings to rubble in the States of Puebla, Morelos and Guerrero, as well as in Mexico City. This second quake occurred at 57 km depth [3] also within the Cocos plate near the northern limit of the Mexican flat-slab [4,5] (see Fig. 1), where it begins to plunge beneath the North American plate, with its epicenter about 120 kilometers from Mexico City and 650 kilometers from Chiapas' M8.2 earthquake [3]. In short, the two quakes happened at two different spots within the Cocos tectonic plate and surprised seismologists [6].

It is the main scope of this paper to show that the occurrence of the aforementioned M8.2 earthquake was not unexpected through analyzing the seismicity in the framework of a new time domain termed natural time χ .

2. Natural time analysis. Background

For a time series comprising N events, we define an index for the occurrence of the k th event by $\chi_k = k/N$, which we term natural time. In this analysis [7,8], we ignore the time intervals between consecutive events, but preserve their order and energy Q_k because we consider that these two quantities are important for the evolution of the system. We, then, study the pairs (χ_k, Q_k) by using the normalized power spectrum $\Pi(\omega) \equiv |\Phi(\omega)|^2$ defined by $\Phi(\omega) = \sum_{k=1}^N p_k \exp(i\omega \chi_k)$, where ω is an angular frequency and $p_k = Q_k / \sum_{n=1}^N Q_n$ is the normalized energy for the k th event, in view of the property of $\Phi(\omega)$ explained below. Upon the occurrence of any additional event, χ_k is “rescaled” as natural time changes to $\chi_k = k/(N+1)$ together with rescaling $p_k = Q_k / \sum_{n=1}^{N+1} Q_n$. In the analysis using natural time, the behavior of $\Pi(\omega)$ is studied at ω close to zero for capturing the dynamic evolution, because all the moments of the distribution of the p_k can be estimated from $\Phi(\omega)$ at $\omega \rightarrow 0$ (see p. 499 of Ref. [9], see also pp. 128–130 of Ref. [7]). For this purpose, a quantity κ_1 is defined from the Taylor expansion

$$\Pi(\omega) = 1 - \kappa_1 \omega^2 + \kappa_2 \omega^4 + \dots, \quad (1)$$

where

$$\kappa_1 = \sum_{k=1}^N p_k \chi_k^2 - \left(\sum_{k=1}^N p_k \chi_k \right)^2, \quad (2)$$

This quantity, which is equal to the variance of natural time, i.e., $\kappa_1 = \langle \chi^2 \rangle - \langle \chi \rangle^2$, is a key parameter that plays an important role in analyzing seismic catalogs [7] for the reasons that will be explained in detail in Section 4. As shown in Ref. [10], at least 6 earthquakes are needed for obtaining one reliable κ_1 value (see also Eq. (2.91) of Ref. [7] where at least six events are needed to differentiate a constant time series, i.e., $Q_k = \text{const.}$ that leads to $\kappa_1 = (1 - 1/N^2)/12$, from the critical behavior observed for Seismic Electric Signals, SES, see Section 4.2, for which $\kappa_1 < 0.08$ according to Eq. (4.37) of Ref. [7]). Natural time analysis when combined with the non-extensive statistical mechanics [11], pioneered by Tsallis [12], enables a satisfactory description of the fluctuations of long term seismicity [13].

The entropy S in the natural time domain is defined [14] as

$$S = \langle \chi \ln \chi \rangle - \langle \chi \rangle \ln \langle \chi \rangle, \quad (3)$$

where the bracket $\langle f(\chi) \rangle = \sum_{k=1}^N p_k f(\chi_k)$ stands for the average value of $f(\chi)$ weighted by p_k , i.e., $\langle \chi \ln \chi \rangle = \sum_{k=1}^N p_k (k/N) \ln(k/N)$ and $\langle \chi \rangle = \sum_{k=1}^N p_k (k/N)$. It is *dynamic* entropy depending on the sequential order of events [15]. The entropy obtained by Eq. (3) upon considering [16] the time-reversal \hat{T} , i.e., $\hat{T}p_k = p_{N-k+1}$, is labeled by S_- , i.e.,

$$S_- = \sum_{k=1}^N p_{N-k+1} \frac{k}{N} \ln \left(\frac{k}{N} \right) - \left(\sum_{k=1}^N p_{N-k+1} \frac{k}{N} \right) \ln \left(\sum_{k=1}^N p_{N-k+1} \frac{k}{N} \right). \quad (4)$$

It was found [16] that, in general, S_- is different from S , and hence S shows the breaking of the time-reversal symmetry. The difference $S - S_-$ will be hereafter labeled ΔS ; this may also have a subscript (ΔS_i) meaning that the calculation is made (for each S and S_-) within a window of length i (= number of successive events), i.e., at scale i see also Section 3. The physical meaning of ΔS has been studied [7,17] using the distribution $P(\chi; \epsilon) = 1 + \epsilon(\chi - 1/2)$ which replaces p_k when considering a continuous variable $\chi \in (0, 1]$ instead of χ_k . Small $|\epsilon| (< 1)$ represents an increase ($\epsilon > 0$) or decrease ($\epsilon < 0$) of Q_k when k increases, thus reflecting the effect of small linear trends in Q_k . It can be shown [7] that $\Delta S(\epsilon) = (\frac{6 \ln 2 - 5}{36})\epsilon + O(\epsilon^3)$ leading to the conclusion that a small increasing trend leads to negative ΔS and vice versa. In addition it has been shown [7] that ΔS_i is probably a key measure which may identify when the system approaches the critical point (dynamic phase transition). For example, ΔS_i has been applied [17] for the identification of the impending sudden cardiac death risk (see also subsection 9.4.1 of Ref. [7]) as well as provides an estimate of the time of its occurrence. (Sudden cardiac death – which may be considered as a dynamic phase transition remains a major cause of death in industrialized countries [18–20].) Furthermore, it has been found that ΔS_i provides a useful tool [21] (see also subsection 8.3.4 of Ref. [7]) to investigate the predictability of the Olami–Feder–Christensen (OFC) model for earthquakes [22], which is probably [23] the most studied non-conservative, supposedly, self-organized criticality (SOC) model (see also [24]). It originated by a simplification of the Burridge–Knopoff spring-block model [25] by mapping it into a non-conservative cellular automaton, simulating the earthquake’s behavior and introducing dissipation in the family of SOC systems. In particular, we found that the value of ΔS_i exhibits a clear minimum [7] (or maximum if we define [21] $\Delta S \equiv S_- - S$ instead of $\Delta S \equiv S - S_-$ used here) before large avalanches in the OFC model, thus this minimum provides a decision variable for the prediction of a large avalanche which corresponds to a large earthquake.

3. Data and analysis

The seismic data analyzed come from the seismic catalog of the National Seismic Service (SSN) of the Universidad Nacional Autónoma de México (www.ssn.unam.mx). To assure catalog completeness a magnitude threshold has been imposed (see also next Section). Since in natural time analysis Q_k should be [7,8] proportional to the energy emitted during the k th earthquake of magnitude M_k , we assumed $Q_k \propto 10^{1.5M_k}$ [7].

In order to estimate the probability density function (PDF) $P(\kappa_1)$ of the κ_1 values in an earthquake catalog, the following steps are taken [7]: Starting from the first event in the catalog, we considered windows of 6 to 40 consecutive events and estimated the corresponding κ_1 values. Starting from the second event, the calculation of the corresponding κ_1 values for 6 to 40 consecutive events has been repeated and so on until the end of the earthquake catalog. This way we obtain a large number of κ_1 values (c.f. when the earthquake catalog comprises of N' events, in total $(N' - 39) \times 35$ κ_1 values are obtained) that enable us to determine their PDF $P(\kappa_1)$ by using standard procedures, e.g., the computer program `histogram` of Ref. [26].

Concerning the calculation procedure for the key quantity of the entropy change under time reversal, a window of length i (= number of successive events) is sliding, each time by one event, through the whole time series. The entropies S and S_- , and therefrom their difference ΔS_i , are calculated each time. Thus, we form a new time series consisting of successive ΔS_i values and search for their extrema which precede the occurrence of a phase change.

4. Results obtained from natural time analysis of seismicity in Mexico

Below, in the first Section 4.1, we summarize the results emerged from the study of the main features of the PDF $P(\kappa_1)$ of the κ_1 values of seismicity, while in the second Section 4.2 we show that in the frame of natural time analysis of seismicity the investigation of the entropy change under time reversal reveals an estimate of the occurrence time of the impending M8.2 earthquake well in advance.

4.1. Results emerged from the features of the PDF $P(\kappa_1)$ of the κ_1 values of seismicity

Earthquakes exhibit complex correlations in time, space and magnitude which have been studied by several authors [27–33]. The observed earthquake scaling laws (e.g., [34]) are widely accepted to indicate the existence of phenomena closely associated with the proximity of the system to a critical point, e.g., [35]. Taking this view that earthquakes are critical phenomena (where a mainshock is the new phase), the quantity by which one can identify the approach of a dynamical system to the state of criticality is termed order parameter. This parameter in the frame of natural time analysis of seismicity is [10] just the quantity κ_1 mentioned in Section 2, as explained in detail in Ref. [10] as well as in pp. 249–254 of Ref. [7]. $P(\kappa_1)$ is constructed by computing the κ_1 values from a natural time window (number of events) sliding through seismic catalogs as described in the previous section. The following two key properties have been shown [7,10]: First is the universality: For different seismic areas $\sigma P(\kappa_1)$ versus $(\mu - \kappa_1)/\sigma$ -where μ stands for the mean of the κ_1 values and σ for their standard

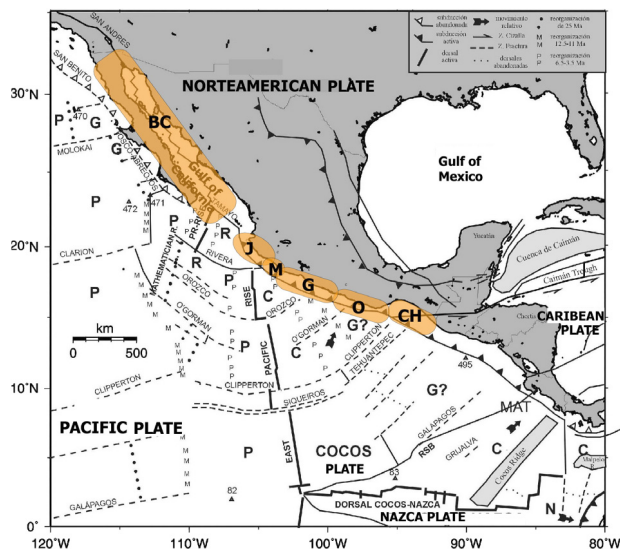


Fig. 2. (Color online) Map showing the six seismic regions studied in Ref. [36].

deviation)- fall on a universal curve which is non-Gaussian (in other words, when studying the order parameter fluctuations of seismicity relative to the standard deviation of its distribution, we find that the scaled distributions of different seismic areas fall on the same non-Gaussian universal curve) [10]. This curve has a left exponential tail which means that an extreme fluctuation may be orders of magnitude more probable than it would be if Gaussian statistics were valid pointing to the existence of extreme events (cf. see Fig. 5 that will be discussed later in which the value $(\mu - \kappa_1)/\sigma = -3.5$ for example corresponds to the value $\sigma P(\kappa_1) \approx 10^{-6.4}$ for a Gaussian distribution (blue curve) while it increases to $\sigma P(\kappa_1) \approx 10^{-4.3}$ for the non-Gaussian distribution depicted by the red curve). Remarkably, such an exponential tail has been also observed in certain critical systems (e.g., 2D Ising, 3D Ising, 2D XY etc.) (see Ref. [10] and references therein). Second, the PDF $P(\kappa_1)$ versus κ_1 before large earthquakes exhibits a bimodal feature. For example, before the Landers M7.3 and before the Hector Mine M7.1 that occurred in Southern California in 1992 and 1999 such a feature appeared (see pp. 274 and 278 of Ref. [7]). Qualitatively similar bimodal feature is also found for temperatures just below the critical temperature T_c in several critical models (see p. 260 of Ref. [7]).

Restricting ourselves to the case of Mexico, the seismicity has been studied in natural time by Ramírez-Rojas and Flores-Márquez in Ref. [36] in the six tectonic regions Baja California (BC), Jalisco-Colima (J), Michoacán (M), Guerrero (G), Oaxaca (O) and Chiapas (CH) of the Mexican Pacific Coast shown in Fig. 2 (the selection of these areas is based on tectonic and geological grounds discussed in Ref. [36]). This study has revealed that only for earthquakes in the three regions CH, G and O out of the six a bimodal feature appears in the PDF $P(\kappa_1)$ versus κ_1 (see their Fig. 3a), thus being candidate areas for the occurrence of large earthquakes. Among these three regions the first one, i.e., CH, the PDF $P(\kappa_1)$ vs κ_1 of which is depicted in Fig. 3, has the highest probability for an extreme fluctuation (large earthquake) as can be seen by comparing their left exponential tail of the $\sigma P(\kappa_1)$ versus $(\mu - \kappa_1)/\sigma$ plot given in Fig. 4, where the results of all six regions are shown while the corresponding results for the CH region can be better visualized in Fig. 5. These results reveal that in principle extreme events, i.e., large magnitude earthquakes, in the Chiapas region have been expected from the natural time analysis. We clarify, however, that the important point here is the strong relation between the criticality shown by the natural time analysis and the occurrence of this large earthquake rather than the “strangeness” of this earthquake in the following sense: Although the natural time analysis would have suggested extreme events in the relevant region, it was apparent that the “extreme” could not correspond to the “strangeness” which seismologists may struggle against, e.g., giant intraplate normal fault.

4.2. Results obtained from the study of the entropy change of the seismicity under time reversal

Aiming at identifying the occurrence time of the major earthquake that struck the Chiapas region, we studied the time evolution of ΔS_i for a number of scales i of the seismicity with $M \geq 3.5$ occurring in this area during the almost six year period 2012–2017. The selection of proper scales i was based on the following grounds: Since $\sim 11,500$ earthquakes ($M \geq 3.5$) occurred in this area from 1 January 2012 until the occurrence of the M8.2 earthquake on 7 September 2017, we find an average of around 170 earthquakes per month. We now consider that recent investigations by means of natural time analysis revealed that the fluctuations of the order parameter of seismicity exhibit [37] a minimum labeled β_{min} when a series of precursory low frequency (≤ 0.1 Hz) electric signals, termed SES activity (e.g., see [38]) initiates. (The lead time of SES activities ranges from a few weeks up to around 5.5 months [7].) While this minimum is observed

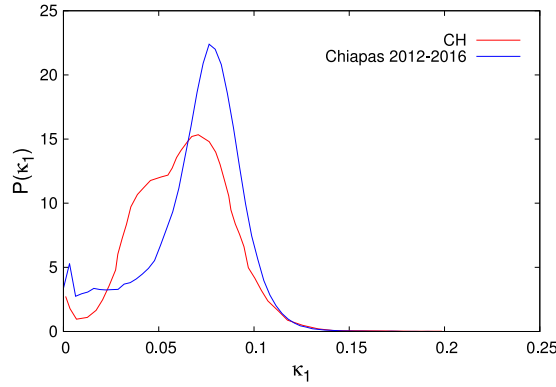


Fig. 3. The PDF $P(\kappa_1)$ versus κ_1 for the region CH (red) during the period 1974–2012 along with the corresponding PDF $P(\kappa_1)$ versus κ_1 (blue) for the same region during the subsequent period 2012–2016. (For interpretation of the references to color in this figure legend, the reader is referred to the web version of this article.)

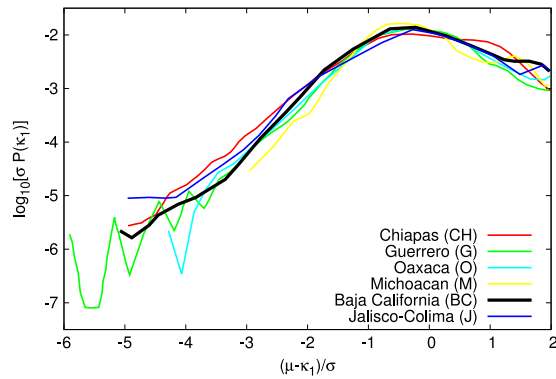


Fig. 4. (Color online) Plot of $\sigma P(\kappa_1)$ versus $(\mu - \kappa_1)/\sigma$ for each of the six seismic regions studied in Ref. [36].

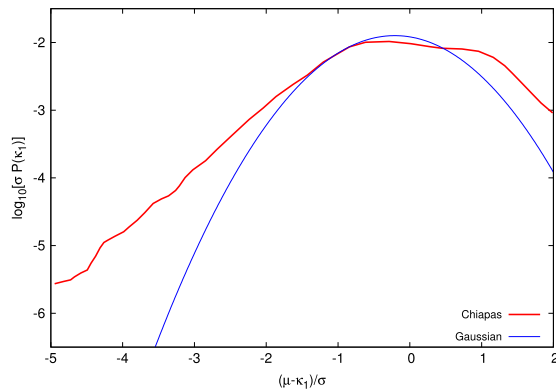


Fig. 5. Plot of $\sigma P(\kappa_1)$ versus $(\mu - \kappa_1)/\sigma$ found in Ref. [36] for the Chiapas region (red). The thin blue line corresponds to a Gaussian distribution and has been drawn as a guide to the eye. (For interpretation of the references to color in this figure legend, the reader is referred to the web version of this article.)

during a period in which long range correlations prevail between earthquake magnitudes, another stage appears before β_{min} in which the temporal correlations between earthquake magnitudes exhibit the distinctly different behavior, i.e., an evident anticorrelated behavior [39]. This significant change between these two stages in the temporal correlations between earthquake magnitudes is likely to be captured by the time evolution of ΔS_i , and this is why we start here the presentation of our study of ΔS_i from the scale of $i \sim 10^3$ events (i.e., around the maximum lead time of SES activities). Thus, we plot in Fig. 6a, b, c, d, e, and f the ΔS_i values versus the number of events for the scales $i = 10^3, 2 \times 10^3, 3 \times 10^3, 3.5 \times 10^3, 4 \times 10^3$ and 5×10^3 events, respectively. Furthermore, for the readers' convenience we also plot in Fig. 7 the values of ΔS_i versus

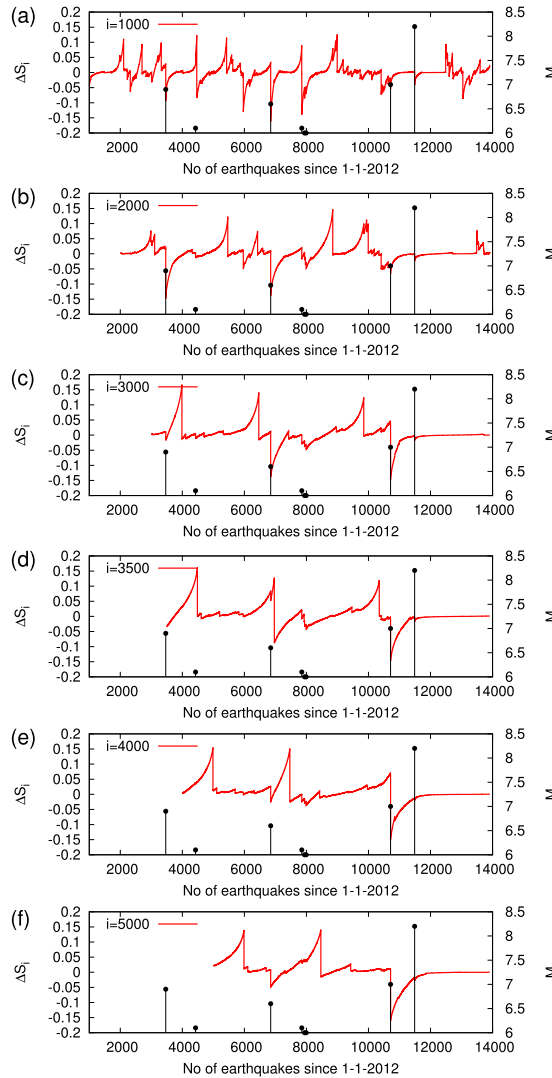


Fig. 6. (Color online) Plot of ΔS_i values versus the number of events. Panels a, b, c, d, e, and f correspond to the scales $i = 10^3, 2 \times 10^3, 3 \times 10^3, 3.5 \times 10^3, 4 \times 10^3$ and 5×10^3 events, respectively, when analyzing all earthquakes with $M \geq 3.5$. The vertical lines ending at circles depict the earthquake magnitudes which are read in the right scale.

the conventional time. Figs. 6 and 7 show that, while at shorter scales a number of (local) minima appear, at longer scales, i.e., $i = 3 \times 10^3, 3.5 \times 10^3, 4 \times 10^3$ and 5×10^3 events, a pronounced minimum becomes evident in Fig. 7 at the date 14 June 2017 (this date can be better visualized in the zoom provided in Fig. 8, which has been plotted only for the period 27 May 2017 to 1 July 2017) which signals that after this date a major event is impending, in a strikingly similar fashion as in the OFC model (see Fig. 8.12 in p. 361 of Ref. [7]). Actually on 7 September 2017, i.e., almost after 3 months, the M8.2 earthquake struck the Mexico's Chiapas state. Such a lead time is of the same order of magnitude with that observed for SES activities and with that of β_{min} identified before all $M \geq 7.6$ earthquakes in Japan during the period from 1 January 1984 until the occurrence of the M9 Tohoku earthquake on 11 March 2011 (note that for this earthquake natural time analysis has been successfully applied to precursory ultra low frequency magnetic field variations [40]). We also note that the date 14 June 2017 of the minimum remains invariant upon changing either the magnitude threshold (e.g., see the results obtained in Fig. 9 for $M \geq 4.0$ instead of $M \geq 3.5$ in Fig. 7) or the scale i for values 3×10^3 events or longer. Such values for the scale do not seem unreasonable if we recall that we have on average 170 earthquakes per month and in addition that there is a widespread belief that the earthquake preparation process starts years before the occurrence of large earthquakes of magnitude 8 or larger (e.g., [41]).

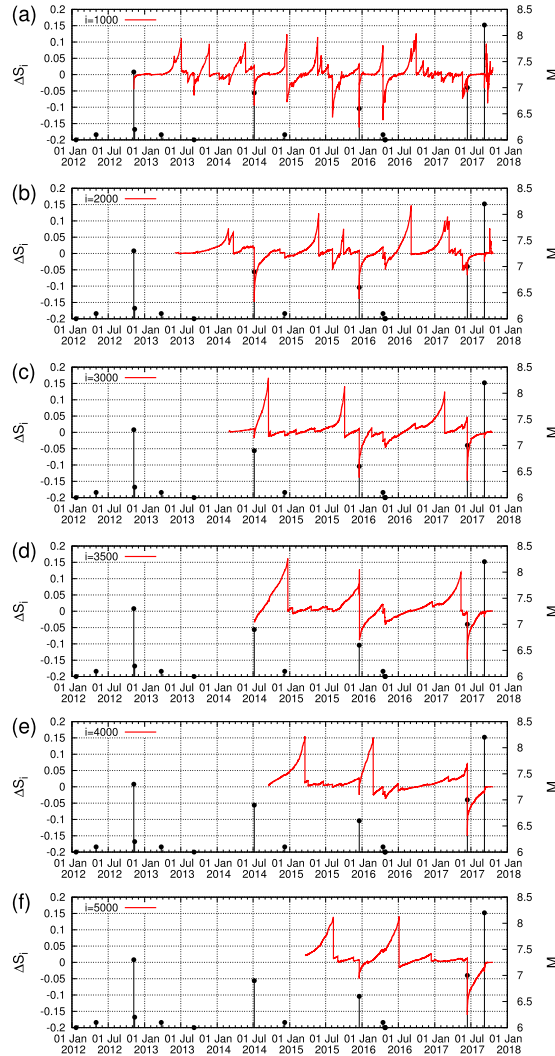


Fig. 7. (Color online) Plot of ΔS_i values versus the conventional time. Panels a, b, c, d, e, and f correspond to the scales $i = 10^3, 2 \times 10^3, 3 \times 10^3, 3.5 \times 10^3, 4 \times 10^3$ and 5×10^3 events, respectively, when analyzing all earthquakes with $M \geq 3.5$. The vertical lines ending at circles depict the earthquake magnitudes which are read in the right scale.

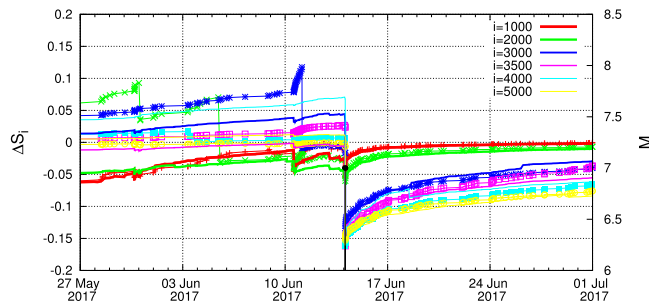


Fig. 8. Plot of ΔS_i values versus the conventional time during the period 27 May 2017 to 1 July 2017. The various continuous lines correspond to the scales $i = 10^3, 2 \times 10^3, 3 \times 10^3, 3.5 \times 10^3, 4 \times 10^3$ and 5×10^3 events when analyzing all earthquakes with $M \geq 3.5$. The points connected with lines result from the natural time analysis of all earthquakes with $M \geq 4.0$ and correspond to the scales $i = 250$ (red), 500 (green), 750 (blue), 875 (magenta), 1000 (cyan) and 1250 (yellow) events as in Fig. 9. The vertical line ending at circle depicts the earthquake magnitude which is read in the right scale. (For interpretation of the references to color in this figure legend, the reader is referred to the web version of this article.)

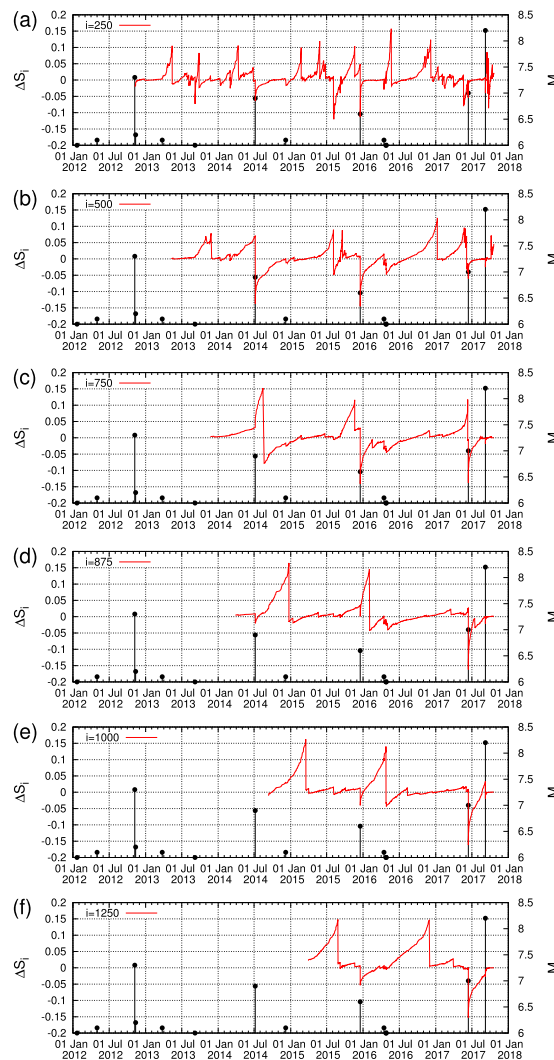


Fig. 9. (Color online) Plot of ΔS_i values versus the conventional time when analyzing all earthquakes with $M \geq 4.0$. Since the number of earthquakes with $M \geq 3.5$ is approximately four times larger than that for $M \geq 4.0$, the scales i presented here are smaller by a factor of 4 compared to Fig. 7, and hence panels a, b, c, d, e, and f correspond to the scales $i = 250, 500, 750, 875, 1000$ and 1250 events, respectively. The vertical lines ending at circles depict the earthquake magnitudes which are read in the right scale.

5. Summary and conclusions

By employing natural time analysis and studying the fluctuations of the order parameter κ_1 of seismicity in six tectonic regions of the Mexican Pacific coast, the following two key properties emerge in the Chiapas region: First, the $P(\kappa_1)$ versus κ_1 plot has a bimodal feature, which signals a forthcoming large earthquake. Second, the feature of the $\sigma P(\kappa_1)$ versus $(\mu - \kappa_1)/\sigma$ plot is non-Gaussian having a left exponential tail. This reflects that the probability for the occurrence of an extreme event is larger by orders of magnitude than it would be if Gaussian statistics were valid. These two key properties seem to support the conclusion that the occurrence of a rare event in this region should not be considered unexpected.

In addition, as far as the occurrence time is concerned, we find that the entropy change under time reversal of the seismicity in the Chiapas area exhibited a clear minimum on 14 June 2017, thus signaling that a major event was impending there as actually happened almost three months later with the occurrence of the M8.2 earthquake on 7 September 2017.

We clarify that the latter minimum on 14 June 2017 of the entropy change under time reversal resulted from the natural time analysis of seismicity solely in the Chiapas region, thus it is related with the M8.2 earthquake on 7 September 2017. Similarly, as for the aforementioned key properties, i.e., non Gaussian feature of the $\sigma P(\kappa_1)$ versus $(\mu - \kappa_1)/\sigma$ plot having a left exponential tail and the bimodal feature of the PDF $P(\kappa_1)$ versus κ_1 plot, they have been found both to be obeyed by analyzing the seismicity in natural time in the Chiapas region, thus they are associated with the large earthquake that occurred in this region on 7 September 2017.

References

- [1] L. Wade, Unusual quake rattles Mexico, *Science* 357 (6356) (2017) 1084. <http://dx.doi.org/10.1126/science.357.6356.1084>.
- [2] E.R. Mega, Deadly Mexico earthquake had unusual cause, *Nature* 549. <http://dx.doi.org/10.1038/nature.2017.22586>.
- [3] A. Witze, Pair of deadly Mexico quakes puzzles scientists, *Nature* 549. <http://dx.doi.org/10.1038/nature.2017.22650>.
- [4] X. Pérez-Campos, Y. Kim, A. Husker, P.M. Davis, R.W. Clayton, A. Iglesias, J.F. Pacheco, S.K. Singh, V.C. Manea, M. Gurnis, Horizontal subduction and truncation of the Cocos Plate beneath central Mexico, *Geophys. Res. Lett.* 35 (18), 118303. <http://dx.doi.org/10.1029/2008GL035127>.
- [5] V. Manea, M. Manea, L. Ferrari, T. Orozco-Esquivel, R. Valenzuela, A. Husker, V. Kostoglodov, A review of the geodynamic evolution of flat slab subduction in Mexico, Peru, and Chile, *Tectonophysics* 695 (Supplement C) (2017) 27–52. <http://dx.doi.org/10.1016/j.tecto.2016.11.037>.
- [6] A. Witze, Deadly Mexico quakes not linked, *Nature* 549 (2017) 442. <http://dx.doi.org/10.1038/549442a>.
- [7] P.A. Varotsos, N.V. Sarlis, E.S. Skordas, Natural time analysis: The new view of time, Precursory Seismic Electric Signals, Earthquakes and other Complex Time-Series, Springer-Verlag, Berlin Heidelberg, 2011. <http://dx.doi.org/10.1007/978-3-642-16449-1>.
- [8] P. Varotsos, N.V. Sarlis, E.S. Skordas, S. Uyeda, M. Kamogawa, Natural time analysis of critical phenomena, *Proc. Natl. Acad. Sci. USA* 108 (2011) 11361–11364. <http://dx.doi.org/10.1073/pnas.1108138108>.
- [9] W. Feller, *An Introduction to Probability Theory and Its Applications, Vol. II*, Wiley, New York, 1971.
- [10] P.A. Varotsos, N.V. Sarlis, H.K. Tanaka, E.S. Skordas, Similarity of fluctuations in correlated systems: The case of seismicity, *Phys. Rev. E* 72 (2005) 041103. <http://dx.doi.org/10.1103/physreve.72.041103>.
- [11] C. Tsallis, Introduction to Nonextensive Statistical Mechanics, Springer, Berlin, 2009. <http://dx.doi.org/10.1007/978-0-387-85359-8>.
- [12] C. Tsallis, Possible generalization of Boltzmann–Gibbs statistics, *J. Stat. Phys.* 52 (1988) 479–487. <http://dx.doi.org/10.1007/BF01016429>.
- [13] N.V. Sarlis, E.S. Skordas, P.A. Varotsos, Nonextensivity and natural time: The case of seismicity, *Phys. Rev. E* 82 (2010) 021110. <http://dx.doi.org/10.1103/physreve.82.021110>.
- [14] P.A. Varotsos, N.V. Sarlis, E.S. Skordas, Attempt to distinguish electric signals of a dichotomous nature, *Phys. Rev. E* 68 (2003) 031106. <http://dx.doi.org/10.1103/physreve.68.031106>.
- [15] P.A. Varotsos, N.V. Sarlis, E.S. Skordas, M.S. Lazaridou, Entropy in natural time domain, *Phys. Rev. E* 70 (2004) 011106. <http://dx.doi.org/10.1103/physreve.70.011106>.
- [16] P.A. Varotsos, N.V. Sarlis, H.K. Tanaka, E.S. Skordas, Some properties of the entropy in the natural time, *Phys. Rev. E* 71 (2005) 032102. <http://dx.doi.org/10.1103/physreve.71.032102>.
- [17] P.A. Varotsos, N.V. Sarlis, E.S. Skordas, M.S. Lazaridou, Identifying sudden cardiac death risk and specifying its occurrence time by analyzing electrocardiograms in natural time, *Appl. Phys. Lett.* 91 (2007) 064106. <http://dx.doi.org/10.1063/1.2768928>.
- [18] J.C. Lopshire, D.P. Zipes, Sudden cardiac death, *Circulation* 114 (11) (2006) 1134–1136. <http://dx.doi.org/10.1161/CIRCULATIONAHA.106.647933>.
- [19] L.R. Dekker, C.R. Bezzina, J.P. Henriques, M.W. Tanck, K.T. Koch, M.W. Alings, A.E. Arnold, M.-J. deBoer, A.P. Gorgels, H.R. Michels, A. Verkerk, F.W. Verheugt, F. Zijlstra, A.A. Wilde, Familial sudden death is an important risk factor for primary ventricular fibrillation, *Circulation* 114 (11) (2006) 1140–1145. <http://dx.doi.org/10.1161/CIRCULATIONAHA.105.606145>.
- [20] D. Müller, R. Agrawal, H.-R. Arntz, How sudden is sudden cardiac death? *Circulation* 114 (11) (2006) 1146–1150. <http://dx.doi.org/10.1161/CIRCULATIONAHA.106.616318>.
- [21] N. Sarlis, E. Skordas, P. Varotsos, The change of the entropy in natural time under time-reversal in the Olami-Feder-Christensen earthquake model, *Tectonophysics* 513 (2011) 49–53. <http://dx.doi.org/10.1016/j.tecto.2011.09.025>.
- [22] Z. Olami, J.S. H.Feder, K. Christensen, Self-organized criticality in a continuous, nonconservative cellular automaton modeling earthquakes, *Phys. Rev. Lett.* 68 (1992) 1244–1247. <http://dx.doi.org/10.1103/physrevlett.68.1244>.
- [23] O. Ramos, E. Altschuler, K.J. Måløy, Quasiperiodic events in an earthquake model, *Phys. Rev. Lett.* 96 (2006) 098501. <http://dx.doi.org/10.1103/physrevlett.96.098501>.
- [24] F. Caruso, H. Kantz, Prediction of extreme events in the OFC model on a small world network, *Eur. Phys. J. B* 79 (2011) 7–11. <http://dx.doi.org/10.1140/epjb/e2010-10635-5>.
- [25] R. Burridge, L. Knopoff, Model and theoretical seismicity, *Bull. Seismol. Soc. Am.* 57 (1967) 341–371.
- [26] R. Hegger, H. Kantz, T. Schreiber, Practical implementation of nonlinear time series methods: The TISEAN package, *Chaos* 9 (1999) 413–435. <http://dx.doi.org/10.1063/1.166424>.
- [27] Q. Huang, Seismicity changes prior to the Ms8.0 Wenchuan earthquake in Sichuan, China, *Geophys. Res. Lett.* 35 (2008) L23308. <http://dx.doi.org/10.1029/2008GL036270>.
- [28] Q. Huang, Retrospective investigation of geophysical data possibly associated with the Ms8.0 Wenchuan earthquake in Sichuan, China, *J. Asian Earth Sci.* 41 (2011) 421–427. <http://dx.doi.org/10.1016/j.jseaeas.2010.05.014>.
- [29] S. Lennartz, V.N. Livina, A. Bunde, S. Havlin, Long-term memory in earthquakes and the distribution of interoccurrence times, *Europhys. Lett.* 81 (2008) 69001. <http://dx.doi.org/10.1209/0295-5075/81/69001>.
- [30] S. Lennartz, A. Bunde, D.L. Turcotte, Modelling seismic catalogues by cascade models: Do we need long-term magnitude correlations? *Geophys. J. Int.* 184 (2011) 1214–1222. <http://dx.doi.org/10.1111/j.1365-246X.2010.04902.x>.
- [31] L. Telesca, V. Lapenna, M. Macchiato, Spatial variability of the time-correlated behaviour in Italian seismicity, *Earth Planet. Sci. Lett.* 212 (2003) 279–290. [http://dx.doi.org/10.1016/S0012-821X\(03\)00286-3](http://dx.doi.org/10.1016/S0012-821X(03)00286-3).
- [32] L. Telesca, M. Lovallo, Non-uniform scaling features in central Italy seismicity: A non-linear approach in investigating seismic patterns and detection of possible earthquake precursors, *Geophys. Res. Lett.* 36 (2009) L01308. <http://dx.doi.org/10.1029/2008GL036247>.
- [33] L. Telesca, Maximum likelihood estimation of the nonextensive parameters of the earthquake cumulative magnitude distribution, *Bull. Seismol. Soc. Am.* 102 (2012) 886–891. <http://dx.doi.org/10.1785/0120110093>.
- [34] D.L. Turcotte, *Fractals and Chaos in Geology and Geophysics*, second ed., Cambridge University Press, Cambridge, 1997.
- [35] J.R. Holliday, J.B. Rundle, D.L. Turcotte, W. Klein, K.F. Tiampo, A. Donnellan, Space-time clustering and correlations of major earthquakes, *Phys. Rev. Lett.* 97 (2006) 238501. <http://dx.doi.org/10.1103/PhysRevLett.97.238501>.
- [36] A. Ramírez-Rojas, E. Flores-Márquez, Order parameter analysis of seismicity of the Mexican Pacific coast, *Physica A* 392 (2013) 2507–2512. <http://dx.doi.org/10.1016/j.physa.2013.01.034>.
- [37] P.A. Varotsos, N.V. Sarlis, E.S. Skordas, M.S. Lazaridou, Seismic electric signals: An additional fact showing their physical interconnection with seismicity, *Tectonophysics* 589 (2013) 116–125. <http://dx.doi.org/10.1016/j.tecto.2012.12.020>.
- [38] P.A. Varotsos, N.V. Sarlis, E.S. Skordas, M.S. Lazaridou, Fluctuations, under time reversal of the natural time and the entropy distinguish similar looking electric signals of different dynamics, *J. Appl. Phys.* 103 (2008) 014906. <http://dx.doi.org/10.1063/1.2827363>.
- [39] P.A. Varotsos, N.V. Sarlis, E.S. Skordas, Study of the temporal correlations in the magnitude time series before major earthquakes in Japan, *J. Geophys. Res.: Space Physics* 119 (2014) 9192–9206. <http://dx.doi.org/10.1002/2014JA020580>.
- [40] M. Hayakawa, A. Schekotov, S. Potirakis, K. Eftaxias, Criticality features in ULF magnetic fields prior to the 2011 Tohoku earthquake, *Proc. Japan Acad. B* 91 (2015) 25–30. <http://dx.doi.org/10.2183/pjab.91.25>.

- [41] S. Tanaka, Tidal triggering of earthquakes prior to the 2011 Tohoku-Oki earthquake (Mw 9.1), *Geophys. Res. Lett.* 39 (2012) L00G26. <http://dx.doi.org/10.1029/2012GL051179>.
- [42] Y. Kim, M.S. Miller, F. Pearce, R.W. Clayton, Seismic imaging of the Cocos plate subduction zone system in central Mexico, *Geochem. Geophys. Geosyst.* 13 (2012), Q07001. <http://dx.doi.org/10.1029/2012GC004033>.